Journal of Physiology (1993), **471**, *pp.* 107–127
With 10 figures
Printed in Great Britain

INACTIVATION OF THE VOLTAGE-DEPENDENT Ca^{2+} CHANNEL CURRENT IN SMOOTH MUSCLE CELLS ISOLATED FROM THE GUINEA-PIG DETRUSOR

BY S. NAKAYAMA AND ALISON F. BRADING
From the University Department of Pharmacology, Mansfield Road, Oxford, OX1 3QT

(*Received 2 December 1992*)

SUMMARY

1. Whole-cell voltage clamp techniques were applied to single smooth muscle cells enzymatically dissociated from guinea-pig urinary bladder. The inactivation and recovery of voltage-dependent Ca^{2+} channel currents were examined by manipulating the membrane potential over a wide range and by changing the extracellular divalent cation concentrations.

2. After exposing the cells to conditioning potentials (−100 to +80 mV in 20 mV increments), the degree of inactivation was estimated by stepping to a 0 mV test potential. In the presence of 2·5 mM Ca^{2+}, the inactivation of the current was U-shaped with respect to the conditioning potential, with maximum inactivation at 0 mV. The maximal inactivation was 60 and 90% after conditioning durations of 0·8 and 5 s, respectively. The U-shaped curve is characteristic of Ca^{2+}-dependent inactivation. When conditioning potentials of +80 mV with either duration were applied, the inward current at the test potential and the subsequent tail current on returning to the holding potential were larger than in control conditions (when the conditioning potential = the holding potential, −60 mV).

3. A U-shaped inactivation curve was also observed in the presence of 2·5 mM Ba^{2+}. The inactivation was maximal with a conditioning potential of about −20 mV, and the inactivation was smaller than seen with Ca^{2+} entry.

4. Paired-pulse protocols were applied to examine the voltage dependence of recovery of the Ca^{2+} inward current. After the inward current had been inactivated during a 100 ms depolarization at 0 mV, it took 700 ms at −60 mV for nearly complete recovery of the current. Recovery was also observed at +80 mV. When the potential of the paired pulses was increased to +20 mV, less recovery was seen when the interpulse potential was at +80 mV. When a longer (3 s) depolarization was applied, the peak amplitude of the inward current took much longer to recover, and had not completely recovered after 4 s at either of the interpulse potentials, although recovery was greater with an interpulse potential of −60 mV than with one of +80 mV. Similar recoveries were observed in the presence of Ba^{2+}.

5. During a long depolarization (8 s, 0 mV), the effects of rapid changes in the extracellular solution were examined. Partial recovery of the inward current occurred after a period in which Ca^{2+} was replaced with Mg^{2+}. This recovery was not observed in the presence of Ba^{2+}. The inward current evoked in the presence of Ba^{2+}

MS 1951

was markedly reduced by substitution of Ba^{2+} with Ca^{2+}. In Ca^{2+}-free solution, if Ca^{2+} was readmitted during a long depolarization, the resulting inward current was larger than the control current at the corresponding time, but smaller than the peak amplitude of the control. The modulation of decay time course by manipulating divalent cations during long depolarizations implies that Ca^{2+}- and voltage-dependent inactivation mechanisms occur separately.

6. Our results suggest that the dominant mechanism involved in Ca^{2+} channel inactivation is Ca^{2+}-dependent inactivation, but voltage-dependent mechanisms are also involved, including the entry of the Ca^{2+} channels into a long, more slowly inactivating open state in response to prolonged depolarization.

INTRODUCTION

Inactivation of the L-type voltage-dependent Ca^{2+} channel current during depolarization is generally observed irrespective of muscle type (Pelzer, Pelzer & McDonald, 1990). Inactivation is normally slow, allowing Ca^{2+} entry during sustained depolarizations to be involved in the regulation of excitation–contraction coupling, co-operating with other activation mechanisms. Two mechanisms of inactivation have been proposed: Ca^{2+}-dependent and voltage-dependent inactivation. Evidence for a Ca^{2+}-dependent mechanism is the U-shaped inactivation that occurs when a wide range of conditioning potentials is used, and the slowing of the decay time course of the Ca^{2+} channel current by injection of Ca^{2+}-chelating agents (Eckert & Tillotson, 1981). Evidence for voltage-dependent inactivation is the inactivation of the Ca^{2+} channel current that occurs if other ions such as Sr^{2+}, Ba^{2+} (Kass & Sanguinetti, 1984; Lee, Marban & Tsien, 1985) or Na^{+} (Hadley & Hume, 1987) are used as charge carriers. Recently, Hadley & Lederer (1991) have shown that these two mechanisms independently inactivate the voltage-dependent Ca^{2+} channels in ventricular myocytes.

L-type Ca^{2+} channels occur in most smooth muscles, but the predominant inactivation mechanisms vary. In Cs^{+}-loaded rat uterine strips, the voltage-dependent Ca^{2+} channel current has been reported to be inactivated by both voltage- and Ca^{2+}-dependent mechanisms (Jmari, Mironneau & Mironneau, 1986, 1987). In various kinds of dissociated smooth muscle cells, Ca^{2+}-dependent inactivation has been shown using patch clamp techniques (guinea-pig taenia caeci: Ganitkevich, Shuba & Smirnov, 1986, 1987; urinary bladder: Ganitkevich & Isenberg, 1991; rabbit portal vein: Ohya, Kitamura & Kuriyama, 1988; canine gastric antrum: Vogalis, Publicover & Sanders, 1992). On the other hand, in smooth muscle cells of guinea-pig ureter (Lang, 1990) and rabbit coronary artery (Matsuda, Volk & Shibata, 1990), a predominant contribution of voltage-dependent inactivation has been reported.

In the preceding paper (Nakayama & Brading, 1993), we have provided evidence that the voltage-sensitive Ca^{2+} channels in smooth muscle cells isolated from guinea-pig bladder enter a second open state (O_2) during depolarization to positive potentials, and that on repolarization these channels, being slow to close, allow a significant tail current of Ca^{2+} to flow into the cell. The presence of this second open state poses two problems with respect to studying inactivation of the channels. Firstly a technical one: when using the conventional two-pulse protocol for

examining channel inactivation, there is the possibility that tail current flowing in the inter-pulse interval may itself cause some inactivation of the voltage-sensitive Ca^{2+} channels, or trigger release of Ca^{2+} from the sarcoplasmic reticulum to enhance inactivation (Sham, Cleemann & Morad, 1992) and thus make it difficult to interpret the results. Secondly, if the second open channel state does not inactivate, or inactivates considerably more slowly than the first open state, then the U-shaped inactivation curves could be caused by a progressive voltage-dependent increase of the population of channels entering the O_2 state during the conditioning depolarization.

In the present study, therefore, we have used other approaches to investigate the inactivating mechanisms that operate in the regulation of voltage-dependent Ca^{2+} channel currents in single smooth muscle cells dispersed from guinea-pig urinary bladder. We have examined inactivation by stepping directly to a test potential from the conditioning potential and have used ranges and durations of conditioning potentials which will activate different amounts of the O_2 channel state. We have also used a concentration jump method to study the inactivating effect of divalent cations at certain potentials. The results revealed that although Ca^{2+}-dependent inactivation is the most important physiologically relevant mechanism for Ca^{2+} channel inactivation in the urinary bladder smooth muscle, there may also be a separate voltage-dependent inactivation, and with large conditioning depolarizations the transformation of the Ca^{2+} channels into a second slowly inactivating long open state clearly plays a role in the U-shaped inactivation curve under these conditions.

METHODS

The methods employed were essentially the same as in the preceding paper (Nakayama & Brading, 1993). Single smooth muscle cells were enzymatically (collagenase and pronase) dissociated from the urinary bladder of male guinea-pigs (400–750 g). Some of the cell suspension was stored at 5 °C before use.

The whole-cell membrane currents were recorded under voltage clamp mode (EPC-7, Germany) through a low-pass filter (10 kHz). The resistance of the patch pipette was in the region of 5 MΩ. The capacitive surge was electrically compensated, and in most experiments, the series resistance was partially compensated (by 50–70 %). Unless otherwise mentioned, the membrane potential was clamped at −60 mV (holding potential). All experiments were performed at room temperature (24–28 °C). An AD/DA converter (DT 2801A, Data Translation, UK) was used for voltage step generation and on-line data acquisition, supported by an IBM compatible computer.

The normal bathing solution had the following composition (mM): NaCl, 125; KCl, 5·9; $CaCl_2$, 2·5; $MgCl_2$, 1·2; glucose, 11·8 and Hepes (*N*-2-hydroxyethylpiperazine-*N'*-2-ethanesulphonic acid), 11·8; pH was adjusted to 7·4 with Tris base. The composition of the pipette solution was (mM): CsCl, 141; $MgCl_2$, 1·4; EGTA (ethyleneglycol-bis-(β-aminoethylether)*N*,*N*,*N'*,*N'*-tetraacetic acid), 2; Hepes/Tris, 10 (pH 7·2). All experiments were carried out at room temperature (24–28 °C). When Ca^{2+} was removed from the bathing solution, Mg^{2+} was increased to 3·7 mM (Ca^{2+}-free, Ba^{2+}-free solution) to keep a constant divalent cation concentration. In Ba^{2+}-containing solution, 2·5 mM Ba^{2+} was added instead of Ca^{2+}. In some experiments, a rapid solution-switching device (Inoue, 1991; Jahr & Westbrook, 1991) was used.

Curve fitting of the decay of the inward currents was done by fitting the discrete data points iteratively with single or multiple exponential functions using a modified 'simplex' program. The total residual currents were used as a criterion for the convergence. At convergence, mean residual currents were usually less than 8 pA.

The numerical data were expressed as means ± S.D. Differences were evaluated by paired or unpaired *t* tests, and a probability of less than 0·05 was taken as a significant difference.

RESULTS

Inactivation of the voltage-dependent Ca^{2+} channel current over a wide voltage range

In Cs^+-loaded single smooth muscle cells of the guinea-pig urinary bladder, inactivation of the voltage-dependent Ca^{2+} channel current was examined over a wide voltage range (−100 to +80 mV). An inactivation curve which can be fitted by a Boltzmann equation is normally obtained with conditioning depolarization of up to 0 mV. However, the use of more positive conditioning depolarizations allowed us to assess how much Ca^{2+}-dependent inactivation contributes to the reduction of the Ca^{2+} channel current, because the inward driving force for Ca^{2+} is negligible at these depolarizations. Investigation of the inactivation of Ca^{2+} channels in the long open state induced by large depolarization (Nakayama & Brading, 1993) was also possible.

Firstly, we used a short conditioning duration to examine inactivation. After exposing the cells to 0·8 s conditioning potentials (−100 to +80 mV in 20 mV increments), the degree of inactivation was estimated by measuring the peak inward current after stepping directly to a 0 mV test potential. Using this protocol, a U-shaped inactivation curve was obtained (Fig. 1). The interval between each voltage sequence was 60–90 s. The inward current evoked by the test potential was not significantly changed by conditioning potentials more negative than the holding potential. However, inactivation occurred with more positive conditioning potentials and was maximal at 0 mV, but only reached 60±9% ($n = 5$). Inactivation decreased with conditioning potentials of more than +20 mV. When a +80 mV conditioning potential was applied, no inactivation occurred, rather, the peak inward current at the test potential was larger (112±5%) and the decay time course was slower than the control obtained after switching to the test potential from −60 mV. This larger current after +80 mV is explained by the greater level of channel activation achieved during the conditioning potential. The tail current evoked by repolarization from the test potential to the holding potential was increased by increasing the conditioning potential to more than 0 mV, suggesting that over this range increasing numbers of channels may be entering the O_2 state.

The effect of prolonging the duration of the conditioning potential to 5 s was examined to see if greater inactivation could be achieved (Fig. 2). Also, it was of great interest to see if the test current had still recovered after positive conditioning potentials in spite of the long conditioning duration (5 s) which is normally considered to achieve a steady state. We found that under these conditions, if the conditioning potential was progressively increased from −100 to +80 mV in 20 mV steps, the inactivation curve was still U-shaped (the maximum at 0 mV), but the inward currents evoked after positive conditioning potentials were depressed compared to control values obtained without a previous conditioning voltage step. The amplitudes of evoked currents were also smaller if shorter intervals (< 30 s) were used between the voltage sequences. When the conditioning potentials were applied in the reverse order, from +80 to −100 mV, the inward currents preconditioned by −60 to −100 mV were much smaller than those evoked after preconditioning at +80 mV. These experiments suggest that the inward currents and inactivation induced by previous voltage sequences have an effect on subsequent currents. For this reason, for the remaining experiments the conditioning potentials were applied in the following order: −60, +80, −80, −100, +60, −40, +40, +20, −20, 0 mV,

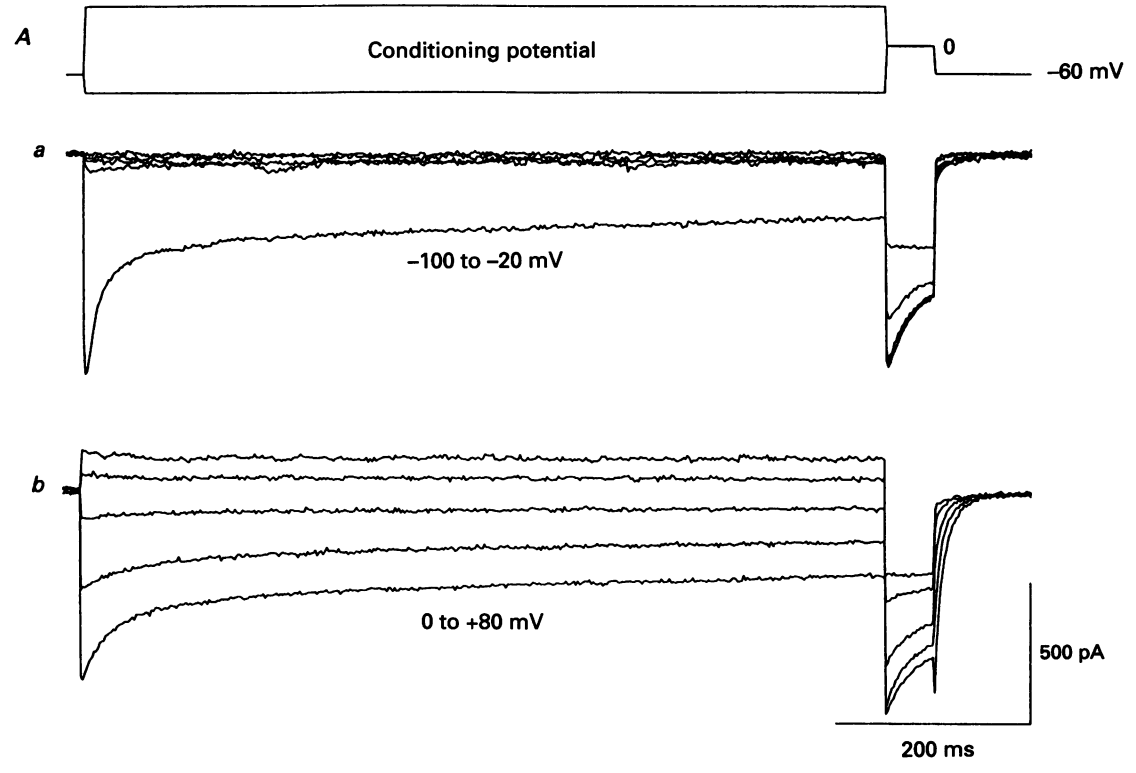

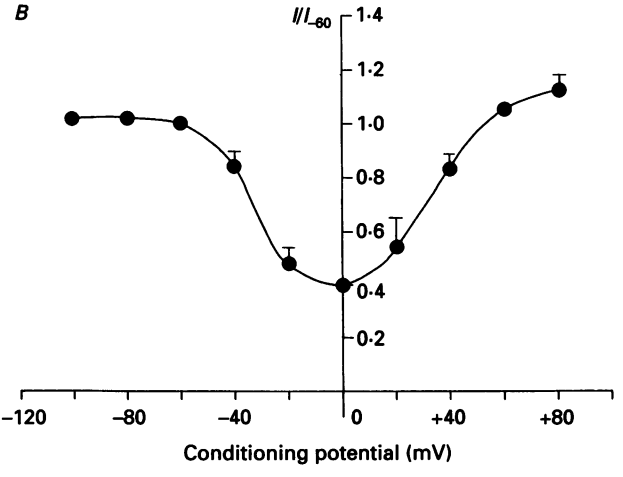

Fig. 1. Voltage dependence of inactivation. After variable conditioning potentials (0·8 s), voltage steps between −100 and +80 mV were applied. Inactivation was estimated from the peak amplitude of the inward current evoked by the following 0 mV test potential (50 ms). *Aa*, current traces for −100 to −20 mV conditioning potentials; *Ab*, current traces for 0 to +80 mV conditioning potentials. *B*, graph showing the relative amplitude of the peak inward current at the test potential. The amplitudes were normalized using each control current preconditioned by −60 mV. Means ± S.D. ($n = 5$).

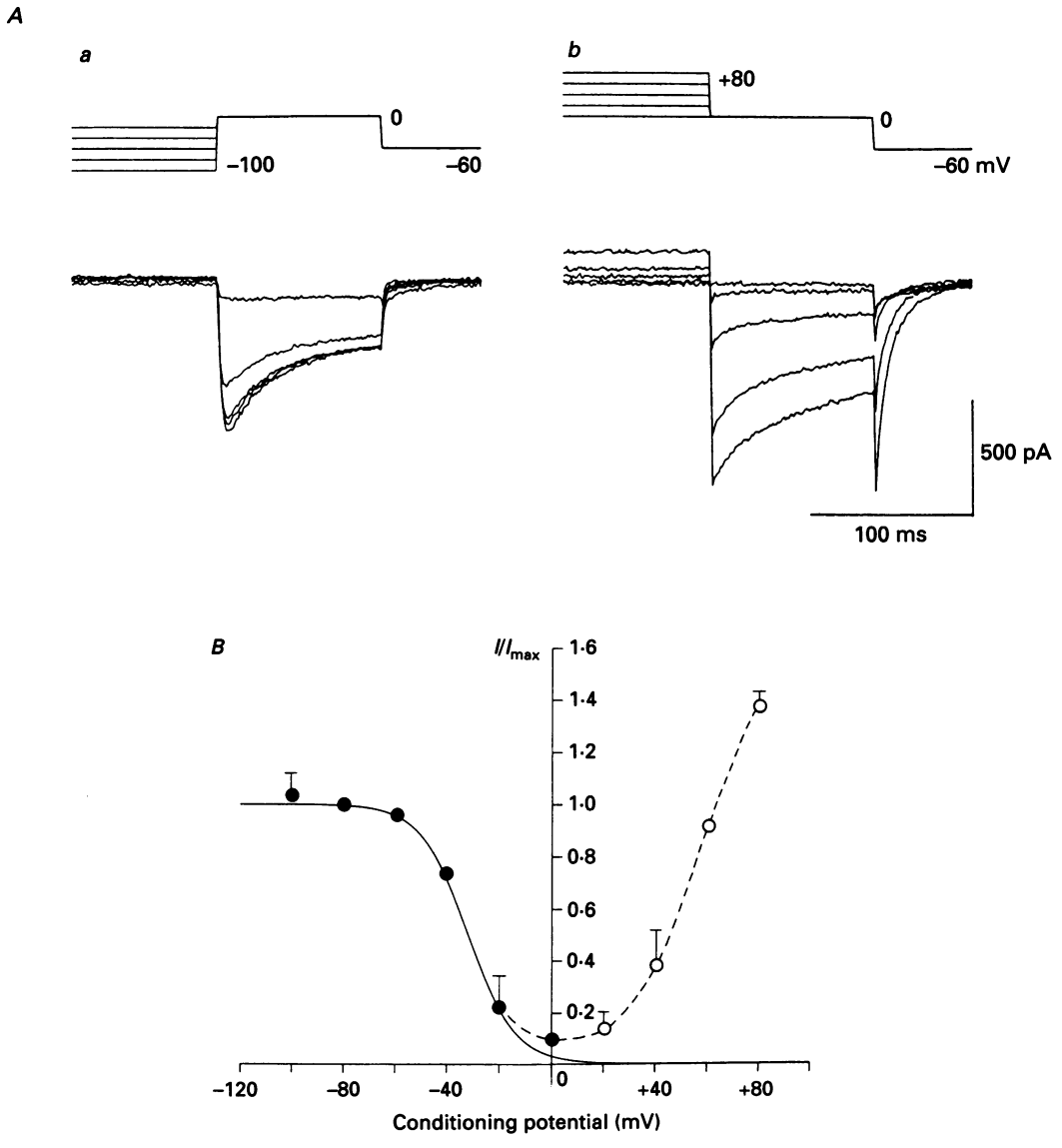

Fig. 2. Effects of long conditioning potentials. The experimental protocol was the same as Fig. 1 except that the conditioning potential was applied for 5 s and the test potential 100 ms. *Aa*, current traces during the test potentials after conditioning potentials from −100 to −20 mV; *Ab*, after 0 to +80 mV conditioning potentials. The last 85 ms of the conditioning potential is shown. The voltage protocol is indicated above the current traces. The various conditioning potentials were applied in the following order (mV): −60, +80, −80, −100, +60, −40, +40, +20, −20, 0 mV. *B*, graph showing the relative amplitude of the peak inward current. Means ± S.D. ($n = 4$). The data obtained by preconditioning potentials of −100 to 0 mV (●) were iteratively fitted by the following equation:

$$I/I_{max} = 1/(1+\exp((E_{0.5})-E)/S)),$$

where $E_{0.5}$ and S are the half-inactivation potential (−31·6 mV) and the slope factor (−9·1 mV), respectively.

and the voltage sequence was repeated at 90–120 s intervals. Using this protocol, we estimate that the effects of the preceding voltage sequence were minimal, and the U-shaped voltage dependence of inactivation (Fig. 2*B*) obtained is probably an accurate reflection of the behaviour of the current. In the range of conditioning potentials between −40 and +60 mV, the inactivation ratios were larger than those shown in Fig. 1*B* in which the conditioning voltage step was of a shorter duration (0·8 s). Maximum inactivation increased to 90±6% ($n = 4$) and still occurred at 0 mV. A conditioning potential of +80 mV both enhanced the amplitude and prolonged the time course of the subsequent inward currents evoked at 0 mV and the tail currents evoked at −60 mV.

When the data obtained with conditioning potentials between −100 and 0 mV were fitted by a conventional Boltzmann distribution, the half-inactivation potential and the slope factor were −31·6 and −9·1 mV, respectively. The half-inactivation potential was more depolarized than that reported for a higher temperature (−38 mV at 35 °C, Klöckner & Isenberg, 1985). This may be explained by augmentation of the inactivation rate by an increase in temperature (Ganitkevich *et al.* 1986; Matsuda *et al.* 1990). The different temperature used may also account for the discrepancy between the present study and that of Ganitkevich & Isenberg (1991) who found that the inward current evoked by a test potential was depressed after a +80 mV conditioning depolarization.

When a double-pulse protocol was used to examine the voltage dependence of inactivation of the Ca^{2+} channel current, the results were rather different. The inward current evoked by a test potential (0 mV) after a +80 mV conditioning pulse (5 s) was significantly smaller than the control obtained without the conditioning pulse. This is in contrast to the increased current seen when a long single preconditioning step was used. With the paired-pulse protocol, this reduction of the inward current after preconditioning at +80 mV occurred even when the conditioning potential was applied directly after the control voltage sequence (−60 mV conditioning), showing that it was not the result of the effects of the preceding sequences. This reduction may be explained by Ca^{2+}-dependent inactivation, as shown below.

Effects of the tail current on the currents evoked by a subsequent depolarization

Figure 3*A* shows a comparison of the inward currents evoked in a cell using the paired-pulse protocol and direct stepping from the conditioning to the test potential. After a 5 s depolarization to +80 mV, the cell membrane was clamped for a further 50 ms either at +80 (*a*), or −60 mV (*b*). A test potential to 0 mV for 100 ms was then applied before returning to the holding potential. Using the paired-pulse protocol, a large inward current was evoked during the first step to −60 mV, and the inward current during the test potential was approximately 40% smaller than seen when directly stepping there from +80 mV. Also there was no tail current when stepping from the test to the holding potential using the paired-pulse protocol, whereas there was a large tail current if the current was stepped sequentially from the conditioning to the test to the holding potential. As the inward currents evoked at the negative membrane potentials are thought to be carried mainly by Ca^{2+}, the reduction of the following inward current at 0 mV may be explained by Ca^{2+}-dependent inactivation of the voltage-dependent Ca^{2+} channel current (Eckert & Tillotson, 1981; Ganitkevich *et al.* 1987). However, it is possible that some deactivation of the

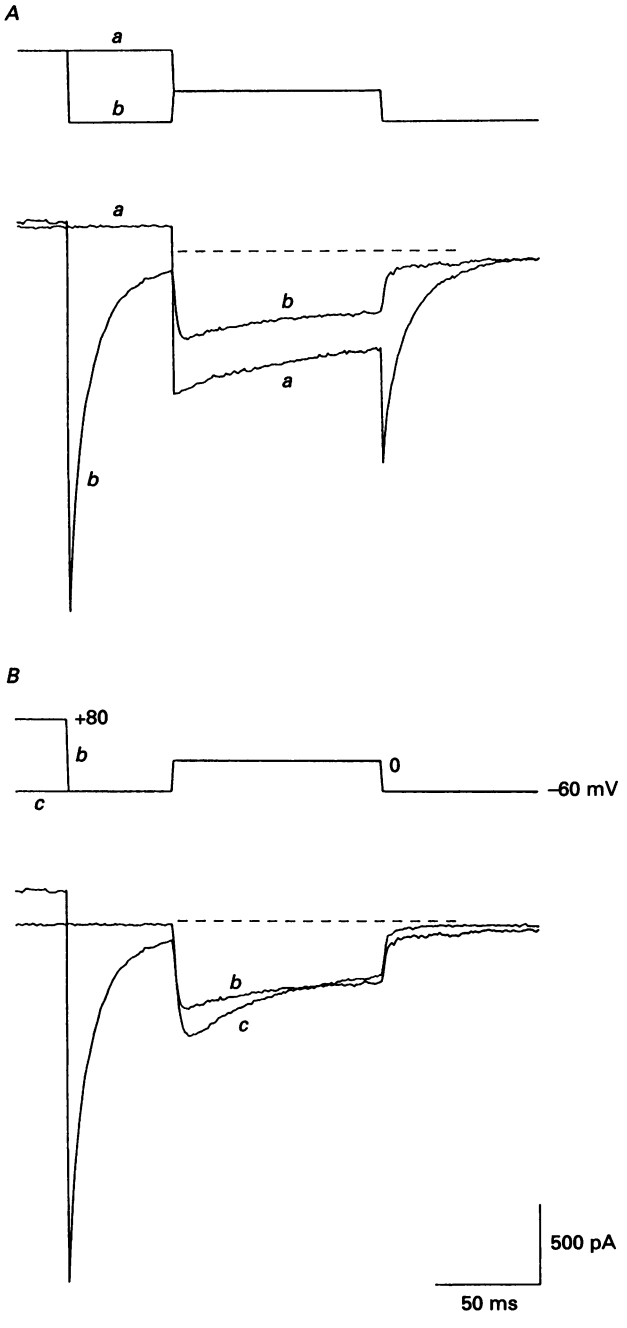

Fig. 3. Effects of the inward tail current on the following depolarization. *A*, after a 5 s conditioning depolarization to +80 mV (last 25 ms shown), the membrane was either held for a further 50 ms at +80 mV (*a*), or stepped for 50 ms to −60 mV (*b*). The latter procedure elicited a large tail current. The membrane potential was then clamped subsequently to 0 mV (100 ms) and then back to the holding potential of −60 mV. The voltage step sequences were applied at 2 min intervals. *B*, the membrane current (*c*) evoked by a simple depolarization (0 mV) is shown, superimposed on *b*. Dashed lines represent the zero current level.

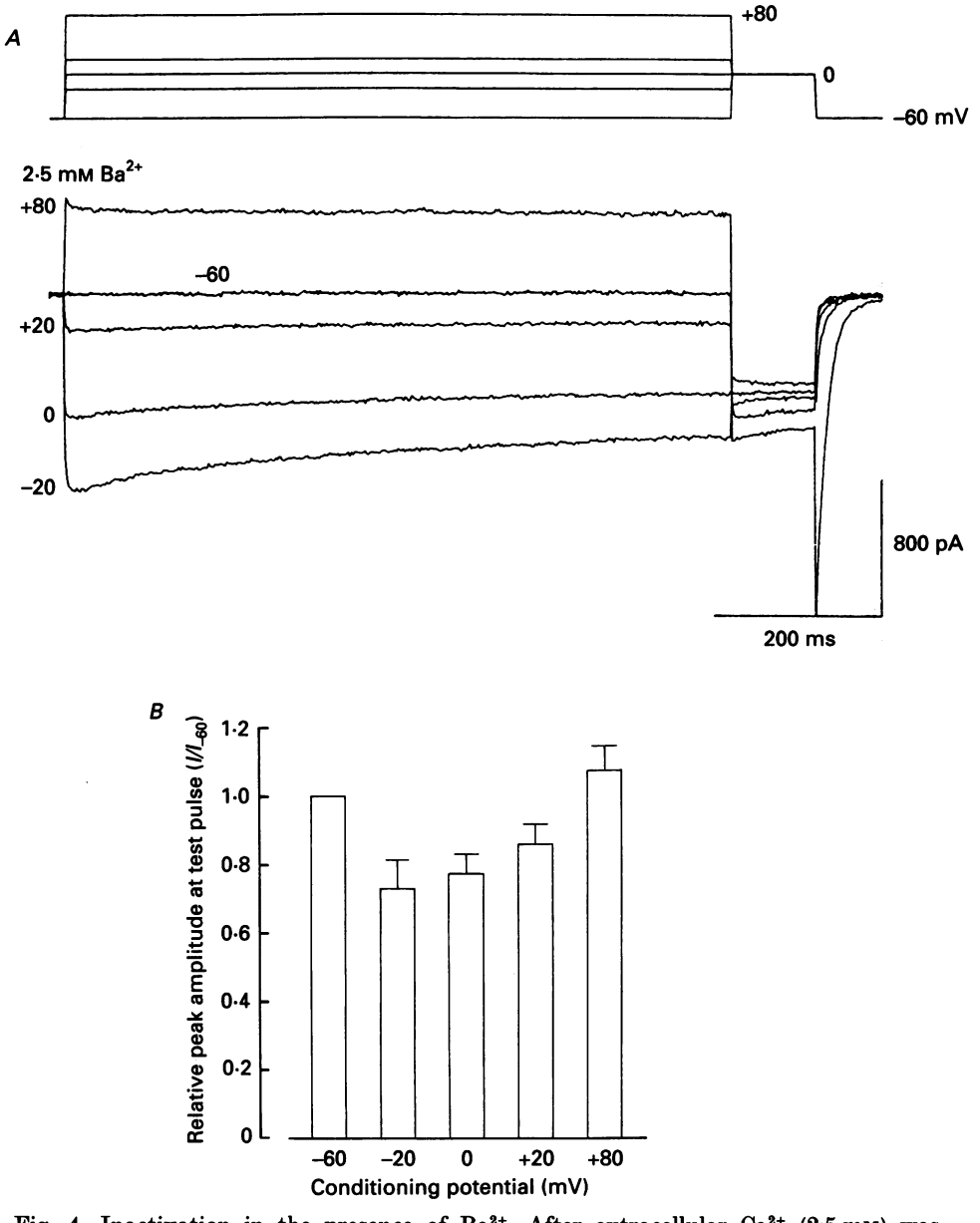

Fig. 4. Inactivation in the presence of Ba^{2+}. After extracellular Ca^{2+} (2·5 mM) was substituted by equimolar Ba^{2+}, the voltage-dependence of inactivation was examined at the 0 mV test potential. The conditioning potentials were applied in the following order (mV): −60, +80, 0, −20, +20 (90 s intervals), *A*, an example of the current traces is shown. *B*, histogram showing the effect of the conditioning potential on the mean peak inward currents at the test potential. The currents are normalized with respect to the control current (preconditioned by −60 mV). Vertical bar, S.D. ($n = 7$). The test columns are all significantly different from the control.

channels occurs during the interpulse interval, and if complete reactivation of the Ca^{2+} channels does not occur at 0 mV (Brading & Nakayama, 1993), this might account for the larger inward current on stepping from +80 mV. Figure 3*B* shows an experiment where current evoked by a simple depolarization to 0 mV (*c*) is

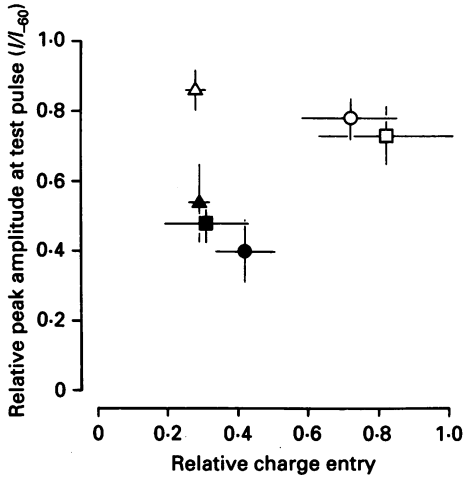

Fig. 5. Graph to show the relationship between degree of inactivation of the test inward current and the charge entry during the preceding conditioning depolarization. Data points from experiments in which the charge carrier was Ca^{2+} are shown as filled symbols, and those with Ba^{2+} as open symbols. □ and ■, data points with conditioning potentials of −20 mV; ○ and ●, 0 mV and △ and ▲, +20 mV. The peak inward current during the test potential (*y*-axis) was plotted against the charge entry (*x*-axis). In each cell, the peak amplitude of the test inward currents preceded by various conditioning potentials was normalized by that evoked after the holding potential (−60 mV step). The total charge entry during the conditioning step (pC) was normalized with respect to the amplitude of the peak inward current (pA = pC/s) evoked by the test potential after conditioning at −60 mV, and therefore had units of s. Means ± S.D., for the *x*- and *y*-axes. In Ca^{2+}-containing solutions, the charge entry and the inactivation are statistically different between −20 and 0 mV, or between 0 and +20 mV.

compared with current evoked by this depolarization after an interpulse interval with a preceding +80 mV conditioning step (as in Fig. 3*Ab*). The peak inward current of *c* was obviously larger than *b*, although the activation level of *c* is probably lower than *b*. These results confirmed Ca^{2+}-dependent inactivation by the inward tail current after a large depolarization.

Inactivation in the presence of Ba^{2+}

Inactivation of the voltage-dependent Ca^{2+} channel was examined in the presence of 2·5 mM Ba^{2+} instead of Ca^{2+} in order to assess the involvement of any voltage-dependent inactivation. As the amplitude of the inward current often gradually decreased during long exposure to Ba^{2+}-containing solutions, only five conditioning potentials of 800 ms were applied at 90 s intervals, to allow comparison with Fig. 1. Figure 4*A* shows an example of the resultant current traces. In the presence of Ba^{2+}, however, inactivation was also U-shaped, although the degree of inactivation was

significantly smaller than in the presence of Ca^{2+}. The maximum inactivation (by $27 \pm 9\%$, $n = 7$) was observed at -20 mV. The conditioning potentials were given in the same order as for Fig. 2, but the degree of inactivation was independent of the order in which the conditioning potentials were applied. The inward current evoked

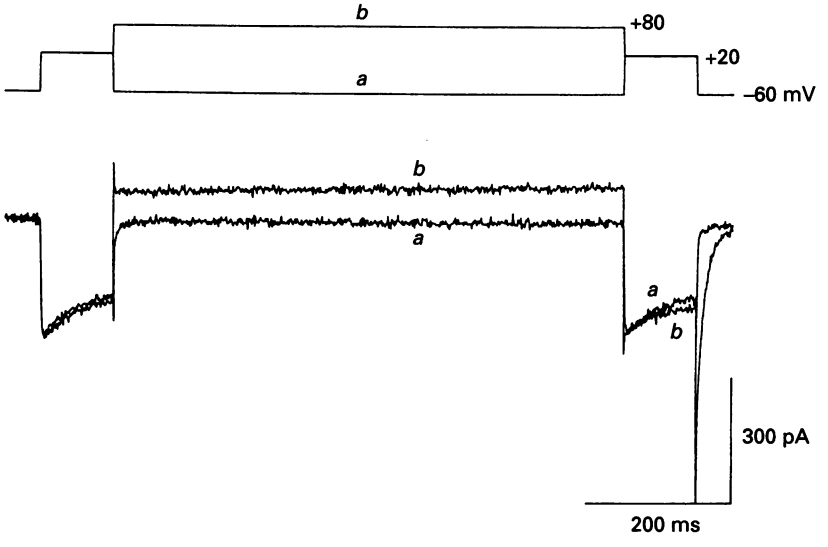

Fig. 6. Effects of interpulse potential on the inward current. Between the paired depolarizations (+20 mV, 100 ms), an interpulse potential of −60 (*a*) or +80 mV (*b*) was applied for 700 ms. The current traces shown were recorded from the same cell.

by the test potential (0 mV) was slightly (7%) larger following a conditioning potential of +80 mV than one of −60 mV; however, the enhancement was smaller than in the presence of Ca^{2+}. After a +80 mV conditioning step, a large tail current was evoked by repolarization to the holding potential of −60 mV, suggesting that Ba^{2+} does not prevent the channels from entering the O_2 state.

In Fig. 5, the degrees of inactivation are compared as a function of charge entry during the conditioning potential between Ca^{2+} and Ba^{2+}. The data shown in Figs 1 and 4 were used. In the presence of either Ca^{2+} or Ba^{2+}, the inactivation was associated with an increase in charge entry. The inactivation was larger when Ca^{2+} was a charge carrier. Maximum inactivation in both cases occurred with maximum charge entries, observed at 0 mV for Ca^{2+} and at −20 mV for Ba^{2+}, suggesting that both Ca^{2+} and Ba^{2+} may be able to produce channel inactivation.

Recovery of voltage-dependent Ca^{2+} channel current

Lack of inactivation of the Ca^{2+} channels during large depolarization has been demonstrated in Figs 1, 2 and 4. It was thus of interest to see if recovery of the Ca^{2+} channels from inactivation can occur during large depolarization. Figure 6 shows the recovery of the inward currents after different interpulse potentials at which little, if any, Ca^{2+} entry will occur. A pair of depolarizing pulses (+20 mV, 100 ms), with a −60 mV interpulse potential, were applied as a control sequence (Fig. 6*a*). The

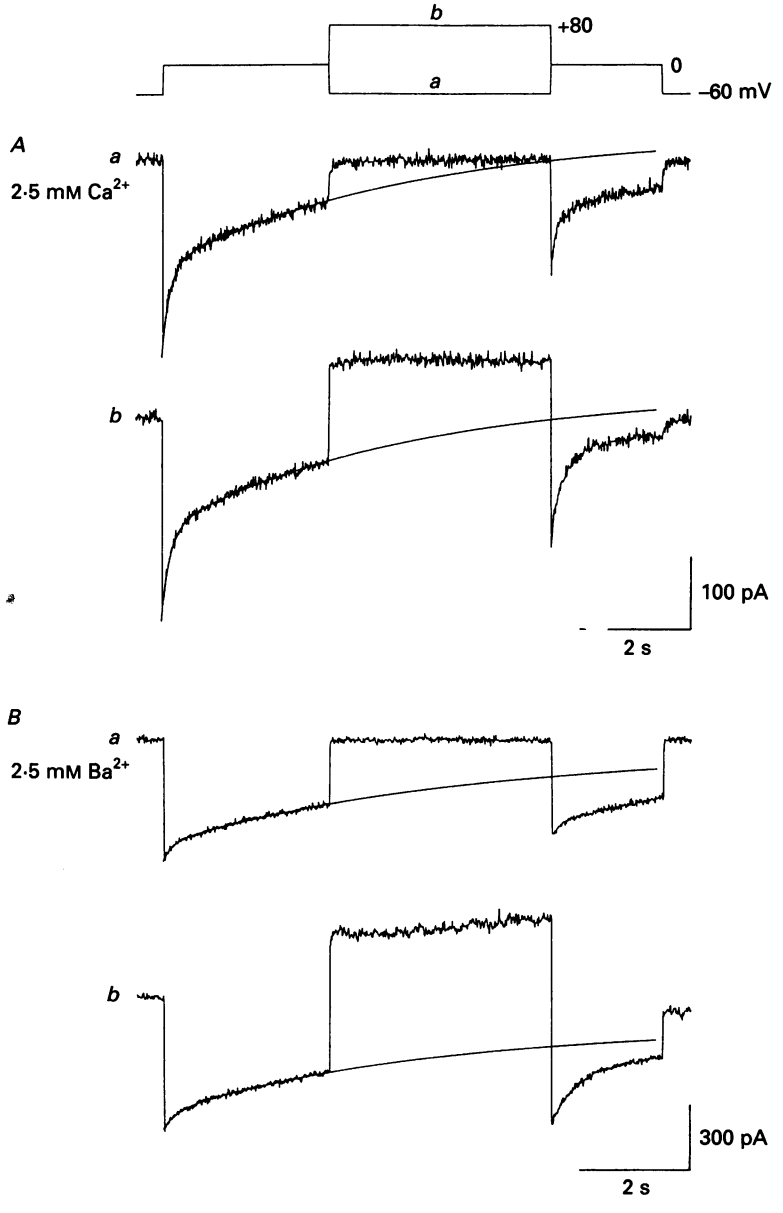

Fig. 7. Recovery of the inward current after a long depolarization in the presence of Ca^{2+} (*A*) and Ba^{2+} (*B*). After a 3 s depolarization (0 mV), the membrane potential was clamped at −60 (*a*) and +80 mV (*b*) for 4 s. At these potentials little Ca^{2+} entry should occur. The recovery from inactivation was estimated from the inward current evoked by the following depolarization (0 mV, 2 s). The membrane current ($I(t)$) evoked during the initial 3 s depolarization was iteratively fitted by a double exponential function:

$$I(t) = A_0 + A_f \exp(-t/T_f) + A_s \exp(-t/T_s),$$

where T_f and T_s were the fast and the slow time constants (ms), respectively and A_0, A_f and A_s are the initial sizes of the non-activating, fast- and slow-inactivating components, respectively. The curve was extrapolated to help show what the current would have been without the intervention. The membrane currents in *A* and *B* were obtained from different cells. The voltage sequence in *a* was applied 2 min after *b*.

inward current evoked by the first depolarizing pulse had declined by the end of the 100 ms pulse to 69±6% ($n = 8$). After a 700 ms interpulse of −60 mV, the peak amplitude of the second inward current had nearly completely recovered (96±2%, $n = 8$), as expected from the recovery time constant (≈ 200 ms, $n = 4$) obtained from preliminary experiments with pairs of pulses with variable interpulse durations. When a +80 mV interpulse potential (700 ms) was applied, recovery of the peak inward current by the second pulse in some cells was identical to that produced by an interpulse potential of −60 mV, but the average of recovery was slightly smaller (87±10%, $n = 8$). This result shows that there is little voltage-sensitive inactivation of the channels during this protocol, and that it is consistent with the suggestion that the recovery is due to the reduction in intracellular Ca^{2+} that will occur during exposure to +80 mV. The subsequent tail current was, however, large, suggesting that a significant number of channels were in the O_2 state (Fig. 6*b*).

Recovery of the inward current from long depolarizations

Three seconds into a long depolarization to 0 mV from a holding potential of −60 mV, the membrane potential was again clamped at an interim potential of either −60 mV or +80 mV, this time for 4 s before returning to 0 mV. Little Ca^{2+} entry into the cell will occur at these two interim potentials, which will allow any effect of the interim potential *per se* to be assessed. Figure 7*A* shows an example of the recoveries that occur during this procedure. During both interim potentials, recoveries in the inward current occurred, but recovery was incomplete after 4 s (61·6±11·7% at −60 mV; 61·4±11·5% at +80 mV, $n = 5$). The decay time course during the first 3 s of the depolarization was fitted by the sum of two exponential terms, and the curve extrapolated to show the inactivation that would have been expected at the time of the second depolarization without the interim change. The same paired recovery protocol was applied using 2·5 mM Ba^{2+} as the charge carrier (Fig. 7*B*), and recovery of inward current was also observed during both interim potentials. It is interesting to note that when either cation was used as the charge carrier, the size of the inward current at the end of the second test potential (0 mV) was larger when the interim potential was −60 mV than when it was +80 mV, suggesting that there may be a voltage-sensitive element to inactivation.

The inactivation during depolarization to 0 mV could be fitted by the sum of two exponential terms when either Ca^{2+} or Ba^{2+} was the charge carrier. In the presence of Ca^{2+}, the fast (T_f) and the slow time constants (T_s) ranged between 70–170 ms and 1·5–4·5 s ($n = 10$), respectively. In the presence of Ba^{2+}, T_f and T_s were 140–380 ms and 3·5–6 s ($n = 6$), respectively. The inactivation time course in the presence of Ca^{2+} could sometimes be fitted better by the sum of three exponential terms, with a faster initial term (current trace not shown). A dissociation of the inward current into three exponential components has also been reported by Klöckner & Isenberg (1985).

Substitution of extracellular divalent cations during depolarization

The experiments so far shown seem to provide evidence for Ca^{2+}-dependent inactivation. However, the presence of more than one open state has also been suggested in this smooth muscle (Nakayama & Brading, 1993). A combination of inactivation of the normal open state and activation to a longer, less readily

inactivated open state, could also result in U-shaped inactivation. Thus the U-shaped inactivation curve alone does not convince us that all inactivation is divalent cation dependent. The following experiments were designed to investigate more precisely the role of divalent cations in inactivation, by changing extracellular

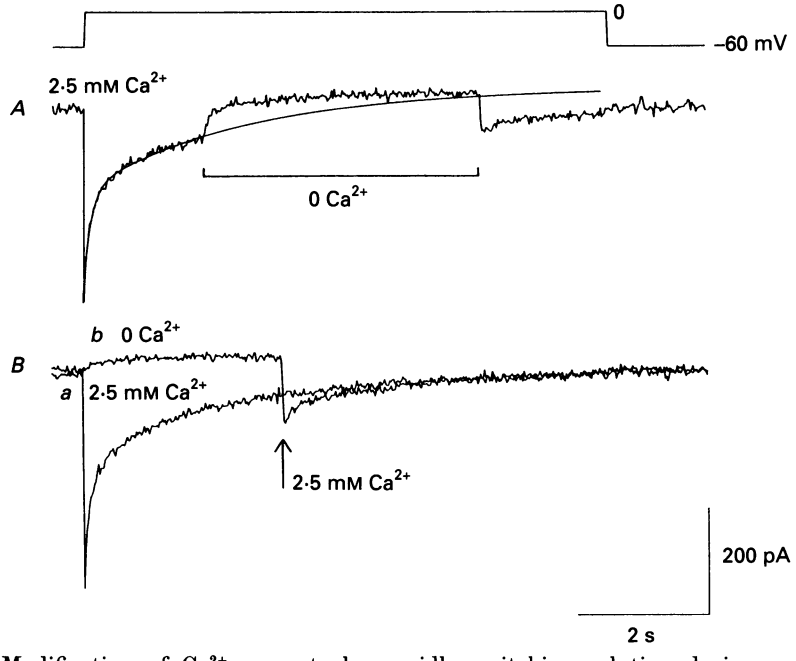

Fig. 8. Modification of Ca^{2+} currents by rapidly switching solution during a long depolarization. In *A*, during an 8 s depolarization at 0 mV, extracellular Ca^{2+} (2·5 mM) was transiently (approximately 4·2 s) removed and replaced with equimolar Mg^{2+}. A double exponential curve was fitted to the inward current before the removal of Ca^{2+}. In *B*, 1 min after the control Ca^{2+} current (*a*) was observed, extracellular Ca^{2+} was removed. Ca^{2+} was readmitted (arrow) during the subsequent depolarization (*b*). The interval between *a* and *b* was 2 min.

divalent cations during a maintained voltage step to a membrane potential (0 mV) at which complete inactivation occurs. In Fig. 8*A*, extracellular Ca^{2+} (2·5 mM) was removed and replaced with equimolar Mg^{2+} for approximately 4 s during depolarization to 0 mV. Ca^{2+} removal completely abolished the inward current evoked by the depolarization. The initial inward current decay (approximately 1·9 s) was fitted by the sum of two exponential terms, and the curve extrapolated to estimate how much the procedure might influence the amplitude of the Ca^{2+} channel current. The readmission of Ca^{2+} resulted in reappearance of the voltage-dependent Ca^{2+} channel current, even though the cell membrane was clamped at a potential which caused the maximum inactivation. Similar recoveries were seen in several other cells, and this again supports the suggestion that recovery from inactivation occurs when intracellular Ca^{2+} declines, and that Ca^{2+} affects the behaviour of the voltage-dependent Ca^{2+} channels during the slow decay time course as well as the initial

phase of depolarization. In Fig. 8*B*, after a control inward current was obtained following a simple, long depolarization (*a*), the cell was exposed to Ca^{2+}-free solution, and the long depolarizing pulse applied again. After 3 s, during the depolarization, extracellular Ca^{2+} was rapidly readmitted (*b*). This resulted in an inward current, the

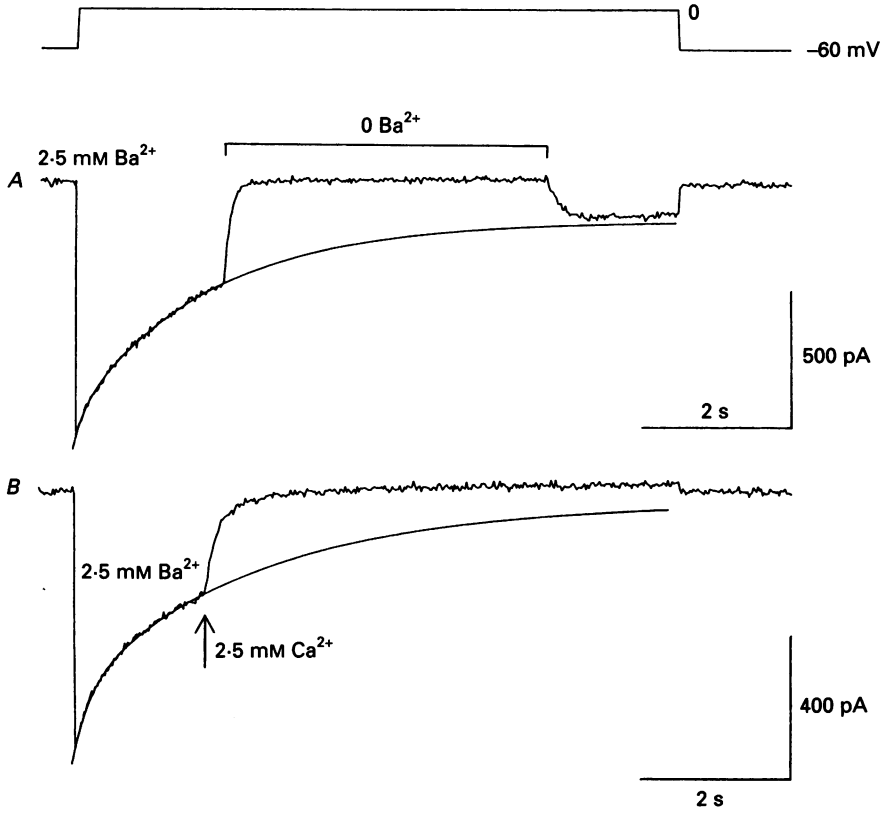

Fig. 9. Modification of Ba^{2+} currents by rapidly switching solution during a long depolarization. In *A*, extracellular Ba^{2+} was transiently removed during the long depolarization (0 mV, 8 s). In *B*, Ba^{2+} was substituted by equimolar Ca^{2+} (arrow). The inward current in the presence of Ba^{2+} was fitted (double exponential) and extrapolated.

peak amplitude of which was larger than the control inward current at the corresponding depolarization time, but smaller than the peak of the control current. In several trials using the same procedure, the peak amplitude of the inward current evoked upon readmission of Ca^{2+} was smaller than the control peak current ($29{\cdot}7 \pm 5{\cdot}1$ % in 6 cells). The fact that the current is smaller, even though no Ca^{2+} will have entered the cell during the depolarization, could be interpreted as suggesting that voltage-dependent inactivation is occurring.

The same long depolarization (0 mV, 8 s) was applied in Ba^{2+} solution (Fig. 9). After about 2 s, extracellular Ba^{2+} was removed and replaced with equimolar Mg^{2+}. The inward current evoked on readmission of Ba^{2+} was no larger than would have been seen if Ba^{2+} had not been removed (*A*), indicating that inactivation is

continuing at this potential, even though Ba^{2+} entry will have stopped. This forms an interesting contrast with the results shown in Fig. 7, where recovery did occur after stepping the potential to +80 mV at which Ba^{2+} entry would be negligible. An explanation for the difference could be that the channels are entering the O_2 state at

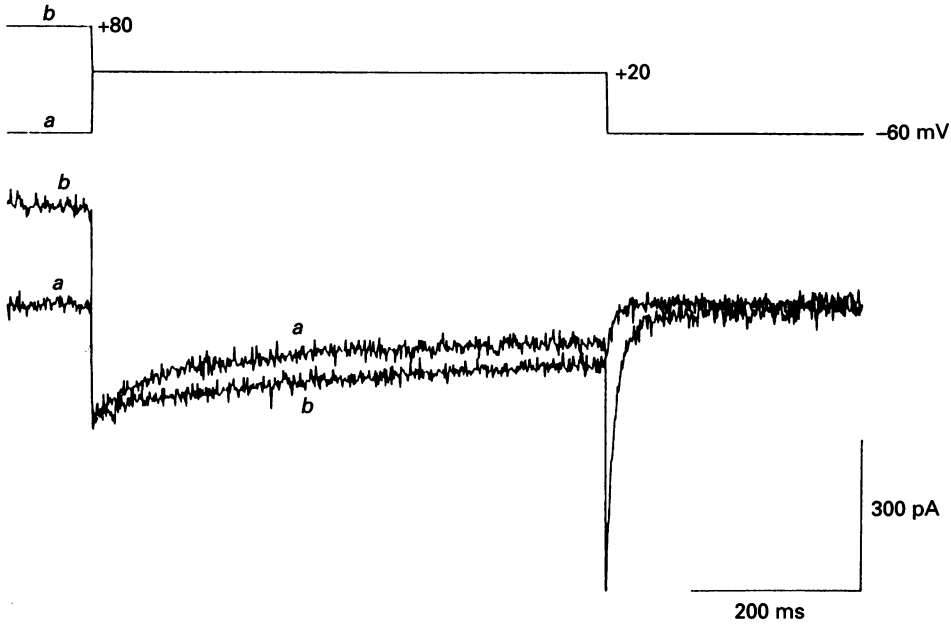

Fig. 10. An example of the contribution of the long open state to the inactivation time course. Unconditioned (*a*) and conditioned (*b*: +80 mV, 5 s) membrane currents were superimposed. A test potential of +20 mV was applied for 600 ms.

+80 mV, and that this state does not inactivate. When Ba^{2+} was replaced by equimolar Ca^{2+} during the long depolarization, the inward current was rapidly reduced (Fig. 9*B*). This large decrease in amplitude cannot be explained solely by the difference in charge-carrying ability of Ba^{2+} and Ca^{2+} at a concentration of 2·5 mM, and seems to be good evidence for Ca^{2+}-dependent inactivation.

Contribution of the long open state

Figure 10 shows an experiment in which the inactivation at +20 mV is compared in unconditioned cells and after a 5 s conditioning potential of +80 mV. This experiment was carried out to see if the O_2 state was inactivated more slowly than the O_1 state. A depolarization to +20 mV (600 ms) was used as the test potential, because at potentials less than this, deactivation from the normal open (O_1) to the closed state would complicate the interpretation. In curve *b*, the population of channels in the O_2 state will have increased during the conditioning potential to +80 mV. The initial amplitudes of the conditioned (*a*) and unconditioned (*b*) inward currents were the same. After 200 ms, the unconditioned current had decayed by 50%, while the conditioned current had decayed by only 32%. Similar results were

reproduced in three more cells. At the +20 mV test potential, an O_2 to O_1 transition will occur, and Ca^{2+} entering the cell will induce Ca^{2+}-dependent inactivation; therefore the conditioned current would be expected to decay. However, the difference in decay time course is good evidence that inactivation of the O_2 state is slower than the O_1 state.

DISCUSSION

In the present study, we have tried to circumvent some of the problems inherent in studying inactivation in the urinary bladder by using various experimental approaches. The uncertainty of a variable contribution to inactivation by Ca^{2+} entering as a tail current in the interpulse interval of the double-pulse protocol was largely avoided by stepping directly from a conditioning potential to a test potential of 0 mV. The other variable was the slow entry of the channels into a second open state which might occur during the conditioning potentials. If this O_2 channel state inactivates more slowly than the O_1 state, it could contribute to the recovery from inactivation at positive potentials.

Direct switching methods have been used by others (e.g. Klöckner & Isenberg, 1985; Smirnov & Aaronson, 1992) to examine inactivation. The main disadvantage is that when the conditioning potential is more positive than the test potential, the degree of activation in the conditioning state can exceed that in the test state. This led to the test inward currents in Figs 1*B*, 2*B* and 4*B* of our experiments being larger after +80 mV than after −60 mV. A short interpulse step in the normal paired-pulse protocols is introduced on the assumption that the channels can be fully deactivated during this step. Because of the transition to the long open state in the bladder (Nakayama & Brading, 1993), deactivation is significantly slowed after positive conditioning potentials, and we judged that direct switching was more appropriate in guinea-pig urinary bladder cells.

Development of the O_2 channel state

To interpret the experiments described in this paper, one needs some idea of how many Ca^{2+} channels are in the O_2 state during any particular protocol. The tail current studies in our previous paper (Nakayama & Brading, 1993) suggest that the O_1–O_2 transition takes a few seconds to reach a steady state. Little activation of the O_2 state occurs at 0 mV, but with further depolarization a significant proportion will shift. A 5 s conditioning depolarization to +80 mV should switch all the available channels into the O_2 state, and the fact that the subsequent test inward current shows no sign of inactivation, strongly suggests that little voltage-sensitive inactivation of the O_2 state can be occurring.

Evidence for divalent cation-dependent inactivation

U-shaped inactivation curves were seen when either Ca^{2+} or Ba^{2+} were used as the charge carrier (Figs 1 and 4). Classically, the reduction of inactivation in normal Ca^{2+} at more positive potentials is interpreted as being caused by a reduced Ca^{2+} entry because of the decreasing driving force near the Ca^{2+} equilibrium potential and is taken as evidence of Ca^{2+}-dependent inactivation. In our experiments, however, it is

clear that if the O_2 channel state does not undergo voltage-dependent inactivation, transition into this state could also contribute to the U-shaped inactivation. Nevertheless, the degree of inactivation we saw with Ca^{2+} as the charge carrier was similar to that obtained in the guinea-pig taenia caeci under similar experimental conditions (Ganitkevich *et al.* 1986). In bladder smooth muscle cells, Ganitkevich & Isenberg (1991) showed an inverse relationship between $[Ca^{2+}]_i$ and the amplitude of the voltage-dependent Ca^{2+} channel current. Very little increase in $[Ca^{2+}]_i$ was observed at +80 mV. The inactivation curve observed in our experiments agrees well with the voltage-dependent increase in $[Ca^{2+}]_i$ described by these authors.

The U-shaped inactivation in the presence of Ba^{2+} was maximum at −20 mV, and was accompanied by the largest charge entry but both were significantly smaller than in the presence of Ca^{2+}. Similar observations have been reported in other smooth muscles (e.g. Vogalis *et al.* 1992). These results could support the idea that Ba^{2+} can bind, albeit with a lower affinity, to the internal binding site to cause divalent cation-dependent inactivation (Markwardt & Nilius, 1988), although again it is possible that the O_1–O_2 transition may have an important role. The development of tail currents in Ca^{2+}-free, Ba^{2+} solution indicates that the O_2 state is still accessible.

Better evidence for Ca^{2+}-dependent inactivation comes from experiments such as those shown in Figs 3 and 9. In Fig. 3 it is clear that Ca^{2+} entry during the tail current can markedly suppress the inward current seen on subsequently stepping to the test potential. In Fig. 9, switching the charge-carrying divalent cation from Ba^{2+} to Ca^{2+} during a long depolarizing pulse to 0 mV causes a rapid switch off of the inward current. Since Ca^{2+} is as effective a charge carrier as Ba^{2+} at a physiological concentration (Nakayama & Brading, 1993), this action of Ca^{2+} is almost certainly due to a rapid inactivation of the voltage-sensitive channels by Ca^{2+} entering the cell.

Evidence for voltage-dependent inactivation

Although the O_2 channel state seems not to undergo significant voltage-dependent inactivation, it is possible that the O_1 state is inactivated both by voltage and $[Ca^{2+}]_i$. Some evidence supporting voltage-dependent inactivation is provided by rapidly changing extracellular divalent cations during long depolarizations to 0 mV where most channels are in O_1. When Ca^{2+} was removed during the depolarization and then readmitted, the inward current disappeared rapidly, and on readmission of Ca^{2+} some 4 s later, the current had recovered, providing evidence for Ca^{2+}-dependent inactivation, but the recovery was not nearly complete (Fig. 8*A*), suggesting that some voltage-dependent inactivation may also be operating. When the experiment was repeated using Ba^{2+} as a charge carrier, no recovery from inactivation was seen in Ba^{2+}-free solution, suggesting that inactivation was mainly voltage dependent. This latter result is in interesting contrast to the experiment shown in Fig. 7, where recovery from inactivation was seen if instead of removing and readmitting Ba^{2+} the membrane potential was stepped to a value of +80 mV, to prevent its entry. This suggests that the recovery at +80 mV may be due more to the O_1–O_2 transition than to a fall in $[Ba^{2+}]_i$, and that Ba^{2+} may not be capable of inactivating the Ca^{2+} channel.

Interaction between voltage- and Ca^{2+}-dependent mechanisms

The reduction of the inward current when Ca^{2+} is readmitted during a long depolarization in Ca^{2+}-free Ba^{2+} solution (Fig. 9*B*), indicates that Ca^{2+}-dependent inactivation can modulate the Ca^{2+} channels at any time during depolarization. It is thus impossible to apply a simple model in which the rapid exponential decay is due to Ca^{2+}-dependent inactivation and the slow phase to voltage-dependent inactivation. The two inactivating mechanisms can probably operate separately, consistent with the conclusion of Hadley & Lederer (1991) from measurements of gating charge in isolated cardiac cells.

The interaction of Ca^{2+}- and voltage-dependent inactivation discussed above is for the O_1 state of the Ca^{2+} channel. The separate operation of these two mechanisms is not clear for the O_2 state, because there is little Ca^{2+} influx at +80 mV. In order to increase intracellular Ca^{2+}, we released Ca^{2+} from intracellular stores with carbachol (0·1 mM). This resulted in a reduction of the inward current at the test potential, and the tail current at −60 mV was also reduced with little change in the decay time course (unpublished observation), suggesting that Ca^{2+} can inactivate the O_2 state.

The effects of long conditioning potentials and window currents

When the conditioning duration was increased from 800 ms to 5 s to allow a steady state to be reached, the amount of inactivation was increased at all conditioning potentials between −40 and +60 mV, and reached a maximum of 90% at 0 mV. Although the data obtained from conditioning potentials of −100 to 0 mV could be fitted by a conventional Boltzmann distribution (Fig. 2*B*), and we have provided some evidence for voltage-dependent inactivation, Ca^{2+}-dependent inactivation is probably more important, depolarization reducing Ca^{2+} entry through non-inactivated Ca^{2+} channels.

Ca^{2+} entry through such channels has been characterized as a 'window current' between the activation and inactivation curves (Klöckner & Isenberg, 1985; Imaizumi, Muraki & Watanabe, 1991; Smirnov & Aaronson, 1992). However, there is some discrepancy between simulated and direct measurements (Aaronson, Bolton, Lang & MacKenzie, 1988) of non-inactivated current or measurements of sustained $[Ca^{2+}]_i$ (Ganitkevich & Isenberg, 1991). The simulation predicts maximal inward current at around −20 mV. Direct measurements have shown that non-inactivated current (or sustained $[Ca^{2+}]_i$) was maximal at more positive potentials. The voltage-dependent development of a long open state (O_2), which inactivates only slowly, or not at all, may be a key to solving this discrepancy.

Conclusions

From our results we would conclude that under normal conditions the most important inactivation mechanism of the inward current is probably Ca^{2+}-dependent inactivation, although a separate voltage-dependent mechanism may also be involved. This Ca^{2+}-dependent mechanism is almost certainly responsible for the inactivation occurring during the action potential. With such short depolarizations the O_1–O_2 transition will not play any role. With longer depolarizations the O_1–O_2 transition may play an increasingly important role in the preservation of the inward

current at more positive potentials, which will flow through the non-, or very slowly inactivating, O_2 channel state.

This work was carried out during the tenure of a grant from Bristol Myers Squibb. The authors are indebted to Dr Derek Terrar for stimulating discussions and also grateful to Drs Narelle Bramich and Ryuji Inoue for helpful comments on the manuscript.

REFERENCES

AARONSON, P. I., BOLTON, T. B., LANG, R. J. & MACKENZIE, I. (1988). Calcium currents in single isolated smooth muscle cells from the rabbit ear artery in normal-calcium and high-barium solutions. *Journal of Physiology* **405**, 57–75.

ECKERT, R. & TILLOTSON, D. L. (1981). Calcium-mediated inactivation of the calcium conductance in caesium-loaded giant neurones of *Aplysia californica*. *Journal of Physiology* **314**, 265–280.

GANITKEVICH, V. YA. & ISENBERG, G. (1991). Depolarization mediated intracellular calcium transients in isolated smooth muscle cells of guinea-pig urinary bladder. *Journal of Physiology* **435**, 187–205.

GANITKEVICH, V. YA., SHUBA, M. F. & SMIRNOV, S. V. (1986). Potential-dependent calcium inward current in a single isolated smooth muscle cell of the guinea-pig taenia caeci. *Journal of Physiology* **380**, 1–16.

GANITKEVICH, V. YA., SHUBA, M. F. & SMIRNOV, S. V. (1987). Calcium-dependent inactivation of potential-dependent calcium inward current in an isolated guinea-pig smooth muscle cell. *Journal of Physiology* **392**, 431–449.

HADLEY, R. W. & HUME, J. R. (1987). An intrinsic potential-dependent inactivation mechanism associated with calcium channels in guinea-pig myocytes. *Journal of Physiology* **389**, 205–222.

HADLEY, R. W. & LEDERER, W. J. (1991). Ca^{2+} and voltage inactive Ca^{2+} channels in guinea-pig ventricular myocytes through independent mechanisms. *Journal of Physiology* **444**, 257–268.

IMAIZUMI, Y., MURAKI, K. & WATANABE, M. (1991). Measurement of noninactivating Ca current in smooth muscle cells. *Methods in Neurosciences* **4**, 44–60.

INOUE, R. (1991). Effect of external Cd^{2+} and other divalent cations on carbachol-activated non-selective cation channels in guinea-pig ileum. *Journal of Physiology* **442**, 447–463.

JAHR, C. E. & WESTBROOK, G. L. (1991). Physiological approaches to the study of glutamate receptors. In *Molecular Neurobiology: A Practical Approach*, ed. CHAD, J. & WHEAL, H., chap. 3, pp. 49–73. Oxford University Press, Oxford.

JMARI, K., MIRONNEAU, C. & MIRONNEAU, J. (1986). Inactivation of calcium channel current in rat uterine smooth muscle: evidence for calcium- and voltage-mediated mechanisms. *Journal of Physiology* **380**, 111–126.

JMARI, K., MIRONNEAU, C. & MIRONNEAU, J. (1987). Selectivity of calcium channels in rat uterine smooth muscles: interactions between sodium, calcium and barium ions. *Journal of Physiology* **384**, 247–261.

KASS, R. S. & SANGUINETTI, M. C. (1984). Inactivation of calcium channel current in the calf cardiac Purkinje fiber: Evidence for voltage- and calcium-mediated mechanisms. *Journal of General Physiology* **84**, 705–726.

KLÖCKNER, U. & ISENBERG, G. (1985). Calcium currents of cesium-loaded isolated smooth muscle cells (urinary bladder of guinea-pig). *Pflügers Archiv* **405**, 340–348.

LANG, R. J. (1990). The whole-cell calcium channel current in single smooth muscle cells of the guinea-pig ureter. *Journal of Physiology* **423**, 453–473.

LEE, K. S., MARBAN, E. & TSIEN, R. W. (1985). Inactivation of calcium channels in mammalian heart cells. *Journal of Physiology* **364**, 395–411.

MARKWARDT, F. & NILIUS, B. (1988). Modulation of calcium channel currents in guinea-pig single ventricular heart cells by the dihydropyridine Bay K 8644. *Journal of Physiology* **399**, 559–575.

MATSUDA, J. J., VOLK, K. A. & SHIBATA, E. F. (1990). Calcium currents in isolated rabbit coronary arterial smooth muscle myocytes. *Journal of Physiology* **427**, 567–680.

NAKAYAMA, S. & BRADING, A. F. (1993). Evidence for multiple open states of the Ca^{2+} channels in smooth muscle cells isolated from the guinea-pig detrusor. *Journal of Physiology* **471**, 87–105.

OHYA, Y., KITAMURA, K. & KURIYAMA, H. (1988). Regulation of calcium current by intracellular calcium in smooth muscle cells of rabbit portal vein. *Circulation Research* **62**, 375–383.

PELZER, D., PELZER, S. & MCDONALD, T. F. (1990). Properties and regulation of calcium channels in muscle cells. *Reviews of Physiology, Biochemistry and Pharmacology* **114**, 107–207.

SHAM, J. S. K., CLEEMANN, L. & MORAD, M. (1992). Gating of the cardiac Ca^{2+} release channel: the role of Na^+ current and Na^+–Ca^{2+} exchange. *Science* **255**, 850–853.

SMIRNOV, S. V. & AARONSON, P. I. (1992). Ca^{2+} currents in single myocytes from human mesenteric arteries: evidence for a physiological role of L-type channels. *Journal of Physiology* **457**, 455–475.

VOGALIS, F., PUBLICOVER, N. G. & SANDERS, K. (1992). Regulation of calcium current by voltage and cytoplasmic calcium in canine gastric smooth muscle. *American Journal of Physiology* **31**, C691–700.